Editors: eLife

LTD at amygdalocortical synapses as a novel mechanism for hedonic learning

Running title: Synaptic mechanisms for CTA learning

Melissa S. Haley, Stephen Bruno, Alfredo Fontanini and Arianna Maffei*

Affiliations. Dept. of Neurobiology and Behavior, SUNY – Stony Brook, Stony Brook, NY

Abstract: 150 words;
Introduction: 490 words;
Discussion: 1949 words
7 Figures;
Methods: 2549 words;

Keywords: insular cortex, LTD, learning, plasticity, taste, conditioned taste aversion

Contributions. All authors were involved in writing and commenting the manuscript.
M.S. Haley designed and performed the experiments, analyzed the data and wrote the manuscript.
S. Bruno performed immediate early genes immunohistochemistry and cell counting.
A. Fontanini obtained funding, designed the study and wrote the manuscript.
A. Maffei obtained funding, designed the study, supervised experiments and analysis, and wrote the manuscript.

Send correspondence to: Arianna Maffei, Dept. of Neurobiology and Behavior, Life Science Building Rm 536, SUNY – Stony Brook, Stony Brook, NY 11794-5230. E-mail: Arianna.maffei@stonybrook.edu

Authors' disclosure: Alfredo Fontanini is a member of the scientific advisory board of Sage Therapeutics, Boston, MA

Acknowledgments: This work was supported by NIH-NIDCD awards DC013770, DC015234 to A. M. and A. F. We wish to thank Dr. Antonello Bonci for useful discussions and feedback on the study.

Abstract

A novel, pleasant taste stimulus becomes aversive if associated with gastric malaise, a form of learning known as conditioned taste aversion (CTA). CTA is common to vertebrates and invertebrates, and is an important survival response: eating the wrong food may be deadly. Previous work reported that CTA depends on the gustatory portion of the insular cortex (GC) and the basolateral nucleus of the amygdala (BLA). However, the synaptic underpinnings of CTA are unknown. Results from molecular and pharmacological studies suggest that CTA is associated with long term potentiation in GC. Differently, experiments in vivo reported decreased activity of GC neurons following CTA. Here we assess the effect of CTA on efficacy and plasticity at the BLA-GC connection. We report that induction of long term depression (LTD) is sufficient to change the hedonic value of a taste stimulus. Our results demonstrate a direct role for amygdalocortical LTD in taste aversion learning.

58 **Introduction**

59 Sensory stimuli are perceived and processed according to their physicochemical and affective
60 signatures. For example, taste perception depends on the chemical identity of a tastant, as well as
61 on its pleasantness or aversiveness (i.e, its hedonic value). Hedonic value can be modulated by
62 experience. Indeed, the affective value of a palatable gustatory stimulus changes if it becomes
63 associated with gastric malaise, a process known as conditioned taste aversion (CTA (Garcia et
64 al., 1955)). In laboratory settings, CTA can be induced in rodents by association of a sucrose
65 solution with gastric malaise caused by an intraperitoneal (ip) injection of lithium chloride. In
66 naïve animals, this association reliably produces a persistent hedonic shift capable of driving
67 avoidance even after a single conditioning trial. Inactivation studies point to the involvement of
68 the gustatory portion of the insular cortex (GC; (Braun et al., 1972; Flynn et al., 1991b; Yamamoto
69 et al., 1995; Cubero et al., 1999)) and the basolateral amygdala (BLA; (Morris et al., 1999)) as key
70 regions necessary for CTA. Evidence from these studies is further corroborated by experiments
71 investigating the interaction between these two regions. In naïve animals, analysis of GC neurons'
72 activity following inactivation of BLA indicates that amygdalar inputs to GC provide information
73 about the affective dimension of taste stimuli (Piette et al., 2012). Recent studies suggest that the
74 expression of aversive behaviors related to taste depend on the output of GC to the amygdala (Lavi
75 et al., 2018; Schiff et al., 2018; Kayyal et al., 2019).

76 While the involvement of GC, BLA and their connections in CTA is well-established, the
77 synaptic changes underlying this form of learning remain unclear. Different experimental
78 approaches produced results that are hard to reconcile. In GC, analysis of molecular markers for
79 synaptic plasticity was brought as evidence that CTA induced long term potentiation (LTP) of GC
80 synapses (Rosenblum et al., 1993; Escobar and Bermudez-Rattoni, 2000; Berman and Dudai,

81 2001; Escobar et al., 2002; Gal-Ben-Ari and Rosenblum, 2011; Rodriguez-Duran et al., 2011;
82 Guzman-Ramos and Bermudez-Rattoni, 2012). Nevertheless, analysis of GC and BLA neurons'
83 spiking activity in awake rodents reported a decrease in firing rate in both regions following CTA
84 (Grossman et al., 2008) – a finding that is inconsistent with the hypothesized induction of LTP.
85 Here we use a combination of immediate early gene immunohistochemistry, patch clamp
86 electrophysiology, and optogenetic stimulation to study plasticity of amygdalocortical circuits in
87 CTA. We demonstrate that CTA reduces activity in GC, and that this decrease is accompanied by
88 long term depression at BLA synapses onto pyramidal neurons in layer 2/3 of GC. Finally, we
89 identify patterns of activity that induce LTD at the BLA-GC input and show that substituting the
90 gastric malaise with this pattern at BLA-GC terminal fields *in vivo* following sucrose consumption
91 is sufficient to reduce the preference for this tastant. Our results provide the first direct evidence
92 that CTA depends on LTD at amygdalocortical synapses, and that this plasticity alters the affective
93 dimension of a sensory stimulus.
94
95 **Results**
96 In order to investigate whether learning induces synaptic plasticity at amygdalocortical
97 synapses in GC, we trained animals in a conditioned taste aversion paradigm where novel,
98 palatable sucrose (0.1M in water) was paired with gastric malaise induced by an intraperitoneal
99 (ip) injection of lithium chloride (LiCl, 0.15M, 7.5mL/kg body weight; **Fig. 1a**). Animals were
100 placed on a water restriction schedule where they received 15 min access to water from a drinking
101 spout in an experimental chamber in the morning, followed by one-hour access to water in their
102 home cages 4 hours later. After four days of habituation, on day 5 and 7, the morning water was
103 replaced with 0.1M sucrose, and the animals received an ip injection of LiCl immediately after

104 consumption. In the control group, pseudo-conditioned animals were exposed to both the US and
105 CS, but they received the LiCl injection the night before sucrose access, and therefore did not form
106 an association between the gastric malaise and tastant. Learning was assessed on day 8 using a 2-
107 bottle test. Average fluid consumption across habituation days for each group was comparable,
108 and animals in both groups initially found the sucrose solution to be palatable, consuming more
109 on the first conditioning day compared to baseline water intake. (**Fig. 1b**; Baseline H_2O, Control:
110 4.29 ± 0.18 mL/day, N = 27; CTA: 4.21 ± 0.16 mL/day, N = 28, control vs. CTA, $p = 0.75$. C1
111 sucrose, Control: 6.58 ± 0.36mL, N=27, vs. H2O, $p < 10^{-8}$; CTA: 6.91 ± 0.31mL, N=28, vs. H2O,
112 $p < 10^{-10}$). However, this preference shifts in the CTA group following the LiCl injection, as
113 indicated by decreased consumption of sucrose on the second conditioning day, and a strong
114 preference for water at testing (**Fig. 1b**; 2-bottle test, Control, sucrose: 7.77 ± 0.34mL, water: 1.46
115 ± 0.24mL, N = 27, $p < 10^{-13}$; CTA, sucrose: 0.65 ± 0.11mL, water: 4.65 ± 0.22mL, N = 28; $p < 10^{-}$
116 ^{14}). A significant difference in the aversion index (AI), calculated as ((water – sucrose)/total
117 volume) (**Fig. 1c**; water preferred for $0 < AI < 1$; sucrose preferred if $-1 < AI < 0$), could be seen
118 in animals in which the exposure to the tastant was followed by an ip injection of LiCl (**Fig. 1c**,
119 CTA, AI: 0.75 ± 0.04, N = 28), compared to animals that received LiCl dissociated from the tastant
120 exposure (**Fig. 1c**, control, AI: -0.69 ± 0.04, N = 27; vs. CTA, $p < 10^{-31}$). Following the 2-bottle
121 test, brain tissue was harvested for either immunohistological processing or acute slice recording
122 experiments. To ensure that the 2-bottle test did not initiate CTA extinction, in a subset of rats we
123 repeated the 2-bottle test on two consecutive days (**Fig. 2a**). Results from the 2-bottle tests (**Fig.
124 **2b**; Water, test 1: 5.41 ± 0.90 mL, test 2: 4.90 ± 1.02 mL, $p = 0.57$; Sucrose, test 1: 0.54 ± 0.15,
125 test 2: 0.47 ± 0.14 mL, $p = 0.77$) and aversion indices on test day and 24 hours later were
126 comparable (**Fig. 2b**; Test 1, AI: 0.77 ± 0.08; Test 2, AI: 0.74 ± 0.08; Test 1 vs Test 2: $p = 0.71$,

N = 8). These results indicate that in our paradigm, CTA was reliably induced, and the 2-bottle test did not initiate an extinction process.

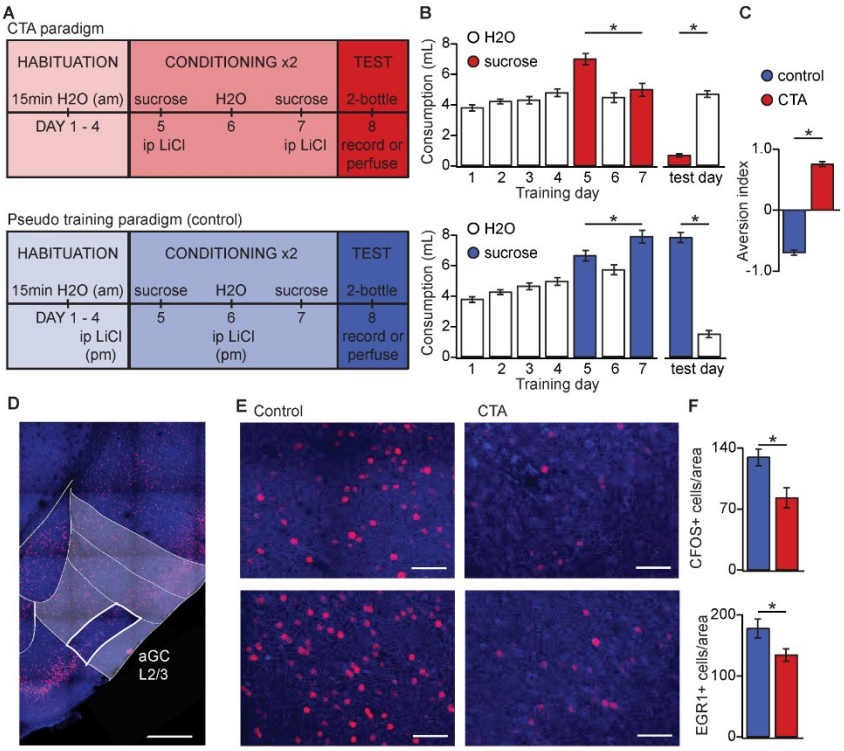

Figure 1: Conditioned taste aversion learning differentially recruits EXC neurons in L2/3 aGC. (A) Behavioral paradigm schematic. Top, red: CTA condition – animals (N = 28) received ip LiCl (7.5mL/kg of 0.15M LiCl) after sucrose exposure. Bottom, blue: Control condition – animals received ip LiCl evening prior to exposure to a sucrose solution. **(B)** Average fluid consumption across training days for each group (outline: H_2O, solid: sucrose; top, red: CTA group, bottom, blue: control group). **(C)** Aversion index on test day for control group (blue) and CTA group (red). **(D)** Representative image depicting region of interest (ROI, L2/3 aGC, white box). Scale bar = 500µm. Red: immediate early gene; blue: Nissl counterstain. For details on imaging procedures see extended Methods. **(E)** Representative images of c-Fos expression (top) and EGR1 expression (bottom) following 2-bottle testing from control group (left) and CTA group (right). Scale bar = 100µm. **(F)** Average counts of c-fos expressing (top, c-Fos: control, blue; CTA, red) and EGR1 expressing (bottom, EGR-1: control, blue; CTA, red) neurons normalized to the area of the ROI. * indicates $p \leq 0.05$. Error bars ± SEM.

144 **Expression of CTA learning results in decreased recruitment of L2/3 EXC neurons.**

145 To begin assessing the effects of CTA on GC, we quantified neurons expressing the activity-
146 dependent immediate early genes (IEGs) c-Fos and EGR1 one hour after the 2-bottle test (**Fig. 1d-**
147 **f**). We focused our analysis on pyramidal neurons in layers 2/3 of GC, as our previous work
148 showed that they receive a powerful input from BLA (Haley et al., 2016). There was a significant
149 decrease in the number of c-Fos and EGR1 positive neurons in the CTA group versus control (**Fig.**
150 **1d-f**; c-Fos, control: 128.13 ± 9.46 positive nuclei/0.1mm^2, N = 6, CTA: 82.21 ± 11.73 positive
151 nuclei/0.1mm^2, N = 6, $p < 0.01$; EGR1, control: 175.90 ± 15.65 positive nuclei/0.1mm^2, N = 6,
152 CTA: 133.03 ± 10.10 positive nuclei/0.1mm^2, N = 6, $p < 0.05$), indicating that expression of the
153 learned aversion to sucrose decreased GC neuronal activation. This effect is consistent with
154 previous reports showing a reduction in GC spiking activity (Grossman et al., 2008).

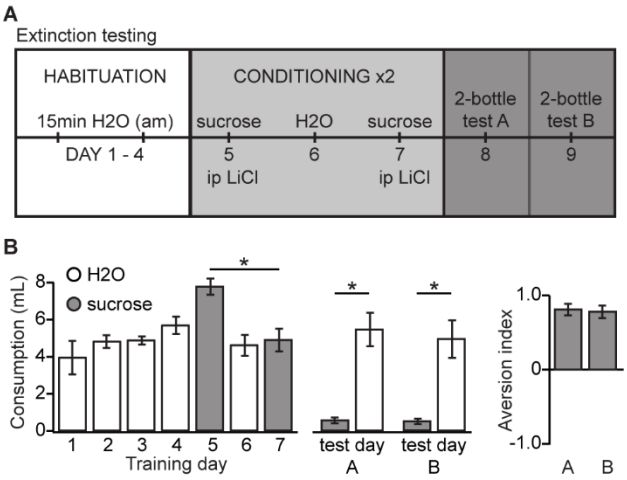

155

156 **Figure 2: Stability of CTA learning across testing days. (A)** Training procedure to assess whether the 2-
157 bottle test does not represent an extinction trial. Top: diagram of behavioral paradigm. **(B)** Left: Average
158 fluid consumption across training session. Middle: Results from 2-bottle tests on two consecutive days.
159 Right: Aversion indices on test day and 24 hours later, N = 8. * indicates $p \leq 0.05$. Error bars ± SEM.

160

161 **CTA learning does not affect the intrinsic excitability of L2/3 pyramidal neurons in GC but**
162 **decreases spontaneous synaptic drive.**

163 The decrease in the number of IEG-labeled neurons following CTA suggests that the
164 associative learning between taste and malaise induced plastic changes in this region of GC, but
165 does not indicate which form of plasticity these changes represent (Inberg et al., 2013; Gandolfi et
166 al., 2017). Indeed, the effect could result from changes to the intrinsic properties of GC neurons,
167 affecting their overall excitability and input/output function. Alternatively, the decrease in
168 expression could be associated with reduced synaptic efficacy, either at specific inputs, such as
169 BLA, or with altered overall synaptic drive onto these neurons.

170 We first assessed the effect of CTA on the input/output function of pyramidal neurons in L2/3
171 of GC. Rats were trained on the control or the CTA paradigm (**Fig. 1a**) starting at postnatal day
172 28 (P28). Following the 2-bottle test, acute slice preparations were obtained for whole-cell patch
173 clamp recordings (Haley et al., 2016). Excitatory neurons were identified online based on their
174 firing response to steady-state current injection, as well as their pyramidal morphology under DIC
175 optics. Recorded neurons were filled with biocytin for post-hoc confirmation of morphology and
176 location, and lack of immunostaining for the GABAergic neuronal marker, GAD-67. All recorded
177 neurons included in the analysis were in L2/3, showed pyramidal morphology, and were negative
178 for GAD67 (**Fig 3a**). To test for possible changes in input/output function, we quantified the
179 frequency of action potentials as a function of the amplitude of injected steady state current steps
180 (FI curve, increments of 50pA). Recordings were performed in the presence of ionotropic receptor
181 blockers (20µm DNQX, 50µm AP5, 20µm picrotoxin) to assess intrinsic membrane properties.
182 CTA did not affect the input resistance (IR) of GC neurons, did not change the action potential
183 threshold (AP), and left the input/output curve unaltered, indicating a lack of changes in intrinsic

properties (**Fig. 3b, c**; input resistance, Control: 149.43 ± 12.98 MΩ, N = 4 rats; n = 19 neurons; CTA: 139.26 ± 10.18 MΩ, p = 0.54, N = 4 rats, n = 19 neurons; AP threshold, Control: -36.38 ± 0.75 mV; CTA: -38.36 ± 0.98 mV, p = 0.10; FI slope, Control: 0.06 ± 0.01; CTA: 0.06 ± 0.01, p = 0.91).

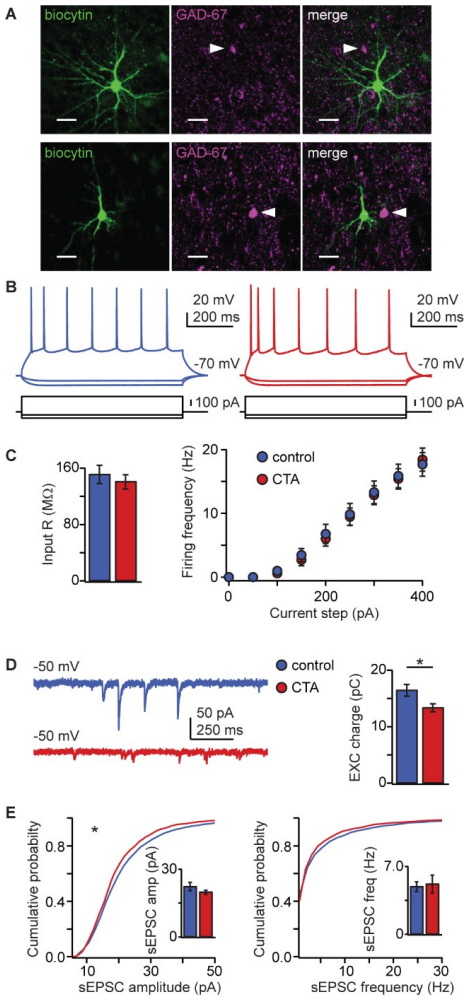

Figure 3: CTA learning does not affect intrinsic excitability but reduces excitatory synaptic drive onto EXC neurons in L2/3 aGC. (A) Images of example recorded neurons from a control animal (top) and CTA animal (bottom). Left: biocytin (green), middle: GAD-67 (magenta), right: Merge showing lack of co-localization. Scale bar = 25µm. **(B)** Steady-state firing patterns of neurons from a. Left: control, blue; right: CTA, red. **(C)** Average input resistance (left) and FI curves (right) for control group (blue) and CTA group (red). **(D)** Left: Sample traces of sEPSCs (holding = -50mV) onto a control neuron (blue) and CTA neuron (red). Right: Summary of EXC charge for control group (blue) and CTA group (red). **(E)** Cumulative probability plots for sEPSC amplitude (left), and sEPSC frequency (right). Insets represent average values for control group (blue) and CTA group (red).* indicates p ≤ 0.05. Error bars ± SEM.

197 These data indicate that following CTA expression, the decrease in the number of GC neurons
198 expressing IEGs is not related to learning-dependent plasticity of intrinsic membrane properties.
199 Next, we examined if the decreased IEG activation following CTA expression could result from
200 changes in synaptic drive. We performed patch clamp recordings in voltage clamp using a cesium
201 based internal solution that allowed for the isolation of spontaneous excitatory (sEPSCs) currents
202 by holding neurons at the reversal potential for chloride (-50mV in our experimental conditions)
203 (**Fig. 3d-e**). Analysis of spontaneous synaptic events unveiled a significant decrease in the
204 cumulative amplitude distribution of spontaneous excitatory synaptic currents (**Fig. 3e**; sEPSCs:
205 K-S test, Control vs CTA: $p < 10^{-6}$; Control: N = 6 rats, n = 22 neurons; CTA: N = 5 rats, n = 22
206 neurons), but no change in their frequency (**Fig. 3e**; sEPSCs: K-S test, Control vs CTA: $p = 0.3$;
207 Control: N = 6, n = 22; CTA: N = 5, n = 22).

208 The decrease in amplitude of spontaneous events was sufficient to result in a significant reduction
209 in spontaneous excitatory synaptic charge (**Fig. 3d**; Control, EXC: 16.3 ± 1.0 pA/ms; N = 6 rats,
210 n = 22 neurons; CTA, EXC: 13.2 ± 0.07 pA/ms; Control vs CTA, EXC: $p < 0.02$). Our results
211 exclude the possibility that CTA altered intrinsic excitability and point to decreased excitatory
212 synaptic transmission as a possible plasticity mechanism for this learning paradigm. Furthermore,
213 given that CTA-induced effects on synaptic drive were detectable in L2/3 pyramidal neurons
214 sampled across the extent of GC, it is highly unlikely for them to depend on selective plasticity on
215 a clustered subset of neurons (Wang et al., 2018b).

216

217 **CTA learning decreases BLA input onto L2/3 pyramidal neurons in aGC**

218 Previous work demonstrated that CTA induction is impaired by inactivation of either GC or
219 BLA (Braun et al., 1972; Bermudez-Rattoni and McGaugh, 1991; Morris et al., 1999), suggesting

220 that the connection between these regions may be a fundamental player in this form of learning.
221 The reduction in the distribution of large events we observed is consistent with the possibility that
222 CTA may affect afferent inputs onto GC neurons, as these typically have larger amplitudes than
223 recurrent events (Wang et al., 2013; Wang et al., 2018a). We therefore asked whether the BLA-
224 GC input onto pyramidal neurons may be affected by CTA. To do that, we used an optogenetic
225 approach to selectively activate BLA terminal fields while recording pyramidal neurons in the
226 superficial layers of GC. As extensively characterized in our previous study (Haley et al., 2016),
227 we injected AAV9.CAG.ChR2-Venus.WPRE.SV40 ((Petreanu et al., 2007); University of
228 Pennsylvania Vector Core; titer: 5.64^{12} particles/mL) in the BLA (2.1 mm posterior to bregma; 4.7
229 mm lateral to midline; 7.0 mm below the pia) of P14 rats. CTA training began 14 days after
230 surgery, at P28. The position of the injection site, and expression of the construct in BLA terminal
231 fields within GC were verified histologically (**Fig. 4a**). Lack of retrograde transport of the
232 construct was verified by the lack of backfilled somata in GC. Consistency of expression across
233 preparations was assessed as indicated in the Methods (**Fig. 4b**), and in our previous work (Wang
234 et al., 2013; Kloc and Maffei, 2014; Haley et al., 2016; Wang et al., 2018a). Following the 2-bottle
235 test, acute slices were prepared (1.5 mm to bregma) and patch clamp recordings were obtained
236 from visually identified L2/3 pyramidal neurons. Brief (5 ms) pulses of blue light (470 nm) were
237 delivered with an LED mounted on the fluorescence light path of an upright microscope and light-
238 evoked excitatory postsynaptic currents (BLA-EPSCs) were recorded. The monosynaptic nature
239 of BLA-EPSCs was verified as described in our previous work (Haley et al., 2016), and an
240 input/output curve for BLA-EPSCs was obtained using light stimuli of increasing intensity (0.2 –
241 4.4 mW, measured at the output of the objective). As shown in **Fig 4c**, BLA-EPSC amplitude was
242 reduced following CTA (**Fig. 4c**; Control: 160.0 ± 22.0 pA, N = 11; n = 29; CTA: 79.5 ± 9.82 pA,

N = 9; n = 27; $p < 0.01$), consistent with the reduction in spontaneous excitatory charge. Furthermore, recordings in current clamp unveiled that the decreased amplitude of BLA-EPSCs resulted in reduced BLA-evoked EPSPs (**Fig. 4c**; Control, BLA-EPSP: 5.82 ± 0.71 mV, N = 11, n = 29; CTA, BLA-EPSP: 3.91 ± 0.44 mV; N = 9, n = 27; $p < 0.05$). As there was no change in input resistance following CTA, the amplitude of BLA-EPSPs shows strong correlation with the amplitude of BLA-EPSCs (**Fig. 4e**; Control: R = 0.77, $R^2 = 0.60$; CTA: R = 0.67 $R^2 = 0.45$; p = 0.43). Since BLA provides a powerful glutamatergic input to L2/3 neurons (Haley et al., 2016), the decrease in BLA-EPSC amplitude strongly suggests that GC neurons are activated less effectively by incoming inputs. This effect may explain the reduced expression of IEGs in **Fig. 1d** and is consistent with reports of decreased GC neurons' activity *in vivo* (Grossman et al., 2008).

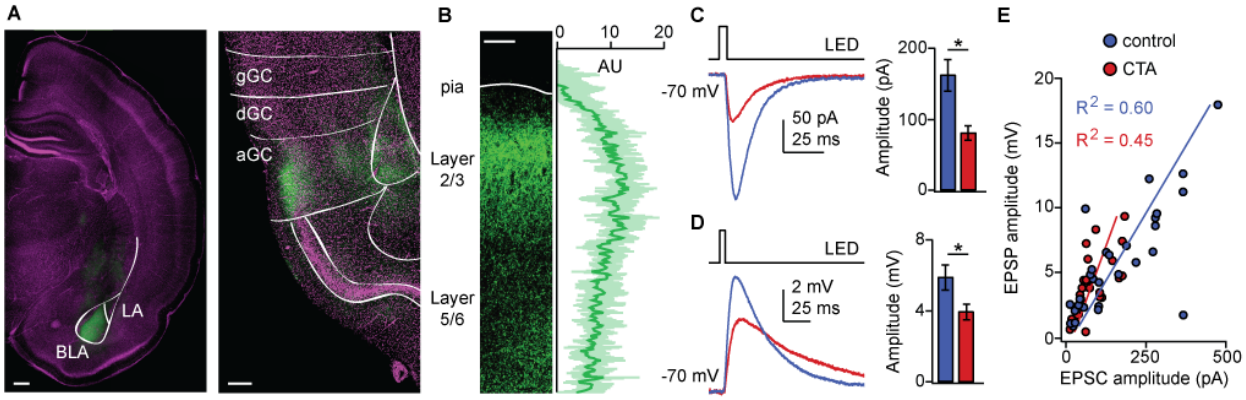

Figure 4: CTA decreases BLA input onto L2/3 pyramidal neurons in aGC. (A) Example of histological verification of injection site and expression of opsin construct in BLA terminal fields in aGC. Left: Image of ChR2-Venus expression at BLA injection site (scale bar = 500µm; BLA, basolateral nucleus; LA, lateral nucleus); right: image of ChR2-Venus expression of BLA afferent fibers in aGC (scale bar = 250µm; green: ChR2-Venus, magenta: Hoechst; gGC, granular GC; dGC, dysgranular GC; aGC, agranular GC). **(B)** Left: Image of ChR2-VENUS expression in BLA afferent fiber in aGC. Scale bar = 250µm. Right: Calibration curve of ChR2-VENUS intensity across lamina in aGC (± 1SD). **(C)** Left: Sample traces of optogenetically-evoked BLA-EPSCs. Right: Summary of BLA-EPSC amplitude onto control neurons (blue) and CTA neurons (red). **(D)** Left: Sample traces of optogenetically-evoked BLA-EPSPs. Right: Summary of BLA-EPSP amplitude onto control neurons (blue) and CTA neurons (red). **(E)** Input-output plot of BLA-EPSCs and BLA-EPSPs for control group (blue) and CTA group (red). * indicates $p \leq 0.05$. Error bars ± SEM.

264 **Induction of LTD at BLA-GC synapses is occluded following CTA learning.**

265 We hypothesized that the decrease in BLA-EPSC may be evidence for induction of long term
266 depression (LTD) at BLA-GC synapses onto L2/3 neurons. We first probed the capacity for
267 plasticity by identifying a pattern of activity that could induce LTD at this input in control animals.
268 We developed induction paradigms consistent with phasic and tonic patterns of BLA neuron
269 activity recorded *in vivo* in awake rodents (Fontanini et al., 2009; Parsana et al., 2012). The effect
270 of such activity patterns on spontaneous GC activity was reported in our previous study (Haley et
271 al., 2016). Patch clamp recordings were obtained from L2/3 neurons in GC of slices obtained from
272 control and CTA rats, prepared right after the 2-bottle test. Following acquisition of a 10min
273 baseline recorded in voltage clamp at -70mV, we paired presynaptic 20Hz bursts of light pulses to
274 activate BLA afferents with depolarization of the postsynaptic GC neuron in current clamp, then
275 continued to record neurons in voltage clamp at -70mV for at least 40 min post-induction. This
276 phasic induction pattern reliably induced LTD at BLA-GC synapses in 56.6% of the recordings
277 from control rats (**Fig. 5b-d**; Control: LTD, % change: 36.63 ± 5.12%, N = 8, n = 13/23). The
278 remaining 43.4% of recordings showed either no change (**Fig. 5b**; Control: no change, 21.7%, N
279 = 4, n = 5/23) or potentiation (**Fig. 5b**; Control: LTP, 21.7%, N = 2, n = 5/23), indicating that BLA-
280 GC synapses are capable of expressing both synaptic depression and potentiation. LTD induced
281 by phasic BLA terminal field activation did not show changes in paired pulse ratio (PPR) nor
282 coefficient of variation (CV) (**Fig. 5c**; Control: PPR, pre: 1.48 ± 0.15; post: 1.20 ± 0.10, N = 8, n
283 = 13, p = 0.09; CV, pre: 0.25 ± 0.04; post: 0.22 ± 0.03, N = 8, n = 13, p = 0.49), indicative of a
284 postsynaptic site of expression (Malinow and Malenka, 2002; Kessels and Malinow, 2009), and
285 consistent with the decrease in amplitude, but not frequency, of sEPSCs shown in **Fig. 3b**.
286

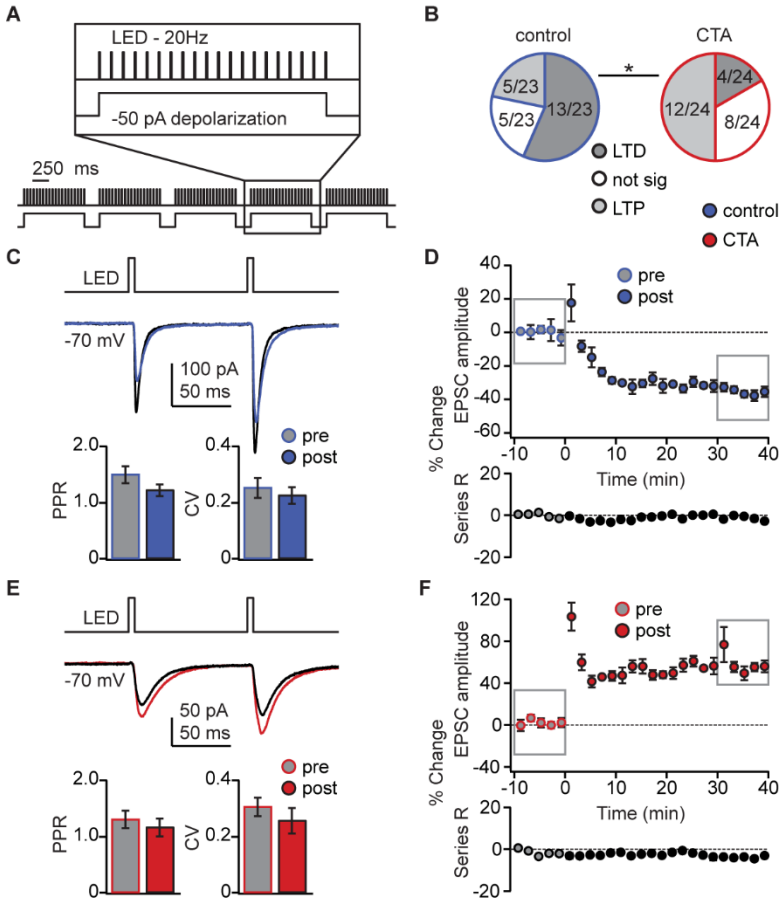

Figure 5. CTA learning occludes LTD induction onto L2/3 pyramidal neurons in aGC. (A) Schematic of 20 Hz plasticity induction paradigm. BLA terminal fields were activated with 20 bursts of 20 light pulses (5ms) at 20Hz delivered every 250ms (Top), while the postsynaptic neuron was depolarized subthreshold by injection of a 50pA current step (Bottom). **(B)** Distribution of the outcome of plasticity induction across all neurons recorded. Left: Control; right: CTA. **(C)** Sample traces of BLA-EPSCs (top) and population PPR (bottom, left,) and CV (bottom, right) before (gray) and after (blue) 20Hz plasticity induction in control group. **(D)** Time course of change in BLA-EPSC amplitude (top) and series resistance (bottom) following 20Hz LTD induction in control group. Boxes indicate pre- and post-induction epochs. **(E)** Sample traces of BLA-EPSCs (top) and summary of PPR (bottom, left) and CV (bottom, right) before (gray) and after (red) 20Hz plasticity induction in CTA group. **(F)** Time course of change in BLA-EPSC amplitude (top) and series resistance (bottom) following 20Hz LTP induction in CTA group. Boxes indicate pre- and post-induction epochs. * indicates $p \leq 0.05$. Error bars ± SEM.

300 We used this induction paradigm to perform an occlusion experiment, testing the possibility
301 that if CTA has saturated LTD at BLA-GC synapses, further LTD induction will result in no
302 additional depression (Rioult-Pedotti et al., 2000; Maffei et al., 2006; Crozier et al., 2007). LTD
303 induction by phasic patterns of BLA terminal field activity in GC was indeed occluded by CTA
304 (**Fig. 5e,f**): the proportion of recordings showing LTD in response to phasic BLA activity was
305 reduced to 16.7% (from 56.6% in control, **Fig. 5b**; CTA: LTD, 16.7%, N = 4, n = 4/24; χ^2 p <
306 0.02), while that of recordings showing LTP increased to 50% (from 21.7% in control, **Fig. 5b,e-**
307 **f**; CTA: LTP, % change: 58.76 ± 10.71%, N = 5, n = 12/24; χ^2 p < 0.01). The proportion of
308 recordings in which induction produced no change in synaptic efficacy was not different from
309 control (**Fig. 5b**; CTA: no change, 33.3%, N = 5, n = 8/24; χ^2 p = 0.13).

310 Similar to the control group, phasic plasticity induction in the CTA group had no effect on
311 either paired pulse ratio or coefficient of variation, consistent with a postsynaptic site of plasticity
312 expression (**Fig. 5e**; CTA: PPR, pre: 1.29 ± 0.16; post: 1.15 ± 0.16, N = 5, n = 12, p = 0.07; CV,
313 pre: 0.30 ± 0.03; post: 0.25 ± 0.05, N = 5, n = 12, p = 0.40). These results strongly suggest that
314 LTD at the BLA-GC synapse is associated with CTA learning.

315 To assess the specificity of the occlusion, we tested the effect of CTA on LTD induction with
316 a different paradigm designed to mimic tonic BLA activity (Fontanini et al., 2009; Parsana et al.,
317 2012) (**Fig. 6a)**. Here, we paired presynaptic ramping light stimuli to tonically activate BLA
318 afferents (Haley et al., 2016), with depolarization of the postsynaptic GC neuron. LTD induction
319 with the tonic BLA activity regime was not occluded by CTA, resulting in LTD in 100% of the
320 recordings in both control and CTA rats (**Fig. 6a-f**; % change, Control: -65.85 ± 6.59 %, N = 2, n
321 = 7/7; CTA: -51.93 ± 11.60 %, N = 2, n = 5/5; control vs CTA: p = 0.66). This form of LTD was
322 accompanied by a significant reduction in paired-pulse ratio, but no changes in coefficient of

variation (**Fig. 6c,e;** PPR: Control, pre: 1.20 ± 0.08; post: 0.93 ± 0.08, N = 2, n = 7, $p < 0.03$; CTA, pre: 1.04 ± 0.02; post: 0.70 ± 0.15, N = 2, n = 5, $p < 0.01$; CV: Control, pre: 0.18 ± 0.02; post: 0.22 ± 0.02, N = 2, n = 7, $p = 0.08$; CTA, pre: 0.19 ± 0.04; post: 0.21 ± 0.04, N = 2, n = 5, $p = 0.34$).

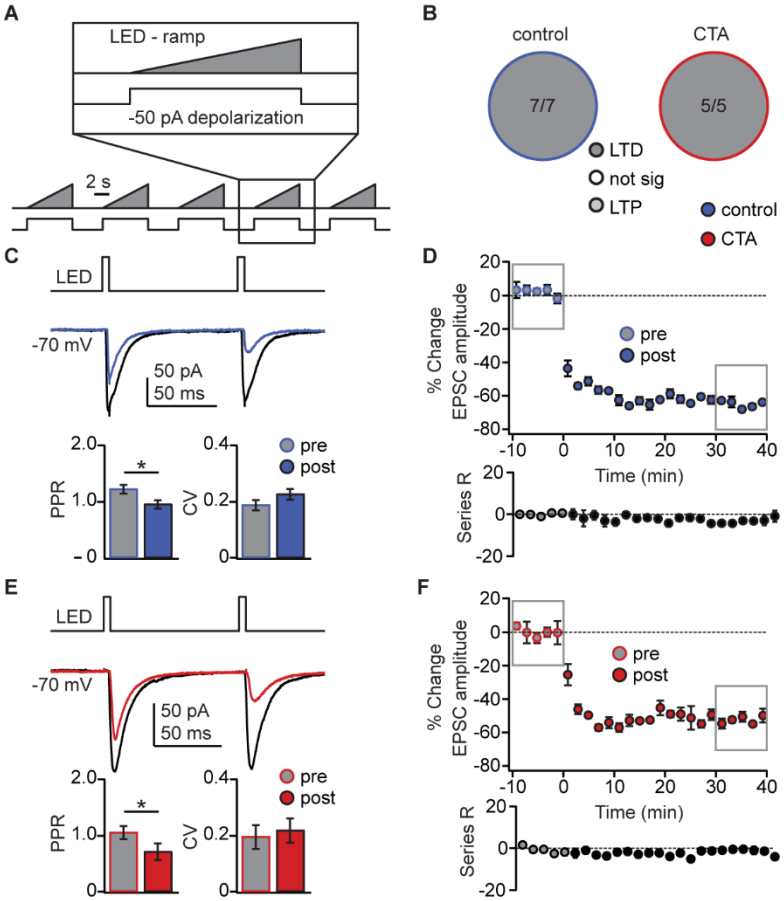

Figure 6: Occlusion of LTD following CTA is specific to BLA activity regime. (A) Schematic of tonic induction paradigm. BLA terminal fields were activated with 6s ramping stimuli delivered every 250ms (Top), while the postsynaptic neuron was depolarized subthreshold by injection of a 50pA current step (Bottom). **(B)** Distribution of the outcome of plasticity induction across all neurons recorded. Left: Control; right: CTA. **(C)** Sample traces of BLA-EPSCs (top) and population PPR (bottom, left,) and CV (bottom, right) before (gray) and after (blue) 20Hz plasticity induction in control group. **(D)** Time course of change in BLA-EPSC amplitude (top) and series resistance (bottom) following tonic LTD induction in control group. Boxes indicate pre- and post-induction epochs. **(E)** Sample traces of BLA-EPSCs (top) and summary of PPR (bottom, left) and CV (bottom, right) before (gray) and after (red) tonic plasticity induction in CTA group. **(F)** Time course of change in BLA-EPSC amplitude (top) and series resistance (bottom) following tonic LTD induction in CTA group. Boxes indicate pre- and post-induction epochs. * indicates $p \leq 0.05$. Error bars ± SEM.

338 This decrease in PPR is consistent with a presynaptic site of plasticity expression, indicating
339 that tonic BLA activity engages a distinct set of plasticity mechanisms that are not consistent with
340 the changes in sEPSC amplitude we observed following CTA. These results strongly suggest that
341 successful CTA learning is associated with postsynaptically expressed LTD induced by phasic
342 activation of BLA afferents in GC.
343
344 **Phasic activation of BLA terminal fields in GC *in vivo* eliminated sucrose preference.**
345 In view of the selective occlusion of LTD induced by phasic BLA terminal field activation, we
346 asked whether association of novel sucrose and phasic activation of BLA terminal fields in GC
347 would be sufficient to change the hedonic value of the tastant. To do that, we injected the
348 AAV9.CAG.ChR2-Venus.WPRE.SV40 construct ((Petreanu et al., 2007); University of
349 Pennsylvania Vector Core) in BLA and implanted an optic fiber (400 μm) in GC (**Fig. 7a**). As
350 control, a group of animals was injected with an AAV9.hSyn.eGFP.WPRE.bGH construct
351 (University of Pennsylvania Vector Core) and implanted with the optic fiber in GC. Both rat groups
352 were trained on a modified CTA paradigm in which the LiCl-induced malaise was substituted with
353 phasic activation of BLA terminal fields (**Fig. 7c**). As shown in **Fig. 7c**, light activation of BLA
354 terminal fields in GC was sufficient to induce a CTA in our experimental group. Whereas both
355 groups showed an initial preference for sucrose over water (**Fig. 7c**; Baseline H_2O, Control: 6.87
356 ± 0.41 mL /day, N = 8; Opto: 7.23 ± 0.21 mL /day, N = 8, Control vs. Opto, p = 0.45. C1 sucrose,
357 Control: 11.60 ± 1.01 mL, N = 8, vs. H2O, $p < 10^{-3}$; Opto: 11.10 ± 1.30 mL, N = 8, vs. H2O, p <
358 0.01), following phasic stimulation, this preference was eliminated in the Opto group, while a very
359 strong preference for sucrose was maintained in the control group (**Fig 7c**; 2-bottle test: Control,
360 sucrose: 12.03 ± 0.73 mL; water: 0.77 ± 0.12 mL; N = 8, $p < 10^{-6}$; Opto, sucrose: 7.91 ± 1.07;

water: 5.35 ± 1.18 mL; N = 8, p = 0.24). The AI measured following optogenetic induction of CTA differed significantly from control (**Fig. 7d**; AI, Control: -0.88 ± 0.01, N = 8; Opto: -0.21 ± 0.15, N = 8; $p < 0.003$), but was lower than that measured across all other CTA training conditions in which LiCl was used to induce the malaise (AI, Opto, **Fig. 7d** vs. CTA, **Fig. 1c**, $p < 10^{-3}$).

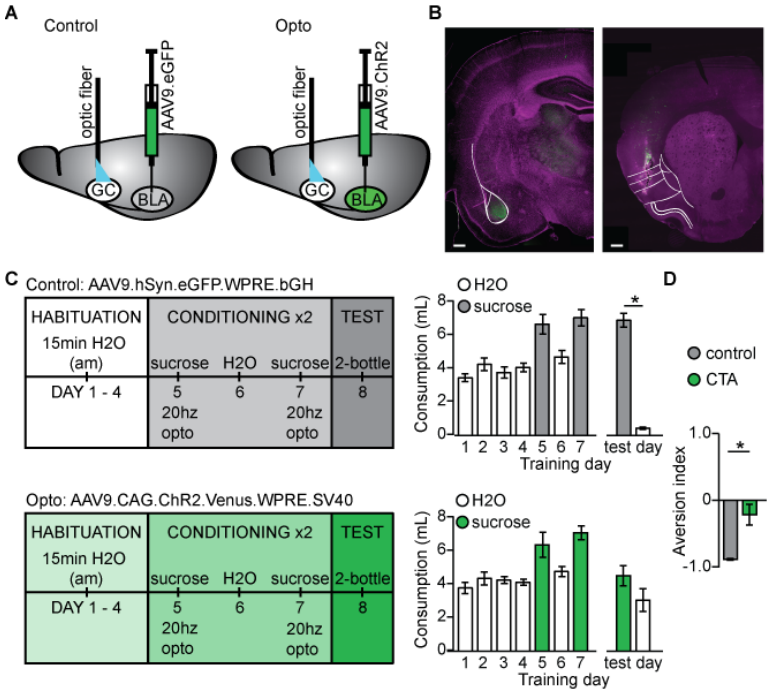

Figure 7: BLA terminal field activation *in vivo* with the phasic 20 Hz pattern eliminated sucrose preference. (A) Cartoon of experimental approach. AAV9.hSyn.eGFP.WPRE.bGH: (Control group) or AAV9.CAG.ChR2-Venus.WPRE.SV40 (Opto group) were injected in BLA and an optic fiber (400 µm diameter, coated with DiL) was implanted in aGC. **(B)** Correct positioning of injection site in BLA and of optic fiber in aGC were verified histologically. Left, green: injection site of ChR2-Venus; magenta: Hoechst counterstain; Right, green DiL indicating optic fiber tract; magenta: counterstain. White lines delineate anatomical landmarks indicating the location of BLA (left) and GC (right) based on the rat brain atlas (Paxinos and Watson, 1998). Scale bar = 500 µm. **(C)** Left: diagram of behavioral paradigm for CTA in which the LiCl injection was substituted with 20 Hz optogenetic stimulation of BLA terminal fields in GC following sucrose exposure. To control for non-specific effects of light stimulation, the training was performed in 2 groups of rats, one injected with an AAV9 construct containing only the fluorescent tag Venus (Control, N = 8 rats) and one injected with the ChR2-Venus construct (Opto, N = 8 rats). Average fluid consumption across training days for each group (outline: H_2O, solid: sucrose; gray: Control group, green: Opto group). **(D)** Right: average aversion index on test day for Control (gray) and Opto (green) rats. * indicates $p \leq 0.05$. Error bars ± SEM.

380 Nevertheless, phasic BLA terminal field stimulation alone changed the preference for the
381 sucrose solution over water, indicating that plasticity at the BLA-GC input is sufficient for altering
382 the hedonic value of a palatable taste stimulus.
383
384 **Discussion**
385 Our data demonstrate that CTA learning leads to reduced activation of the taste responsive portion
386 of the insular cortex and to an LTD-related reduction in strength of the BLA-GC connection. The
387 results also demonstrate that induction of LTD at amygdalocortical synapses onto L2/3 pyramidal
388 neurons is sufficient for changing the hedonic value of a taste stimulus. These findings, which
389 confirm the central role of the projection from BLA to GC in CTA, also reveal that circuit changes
390 following CTA learning do not depend, as previously thought, on strengthening of synaptic
391 connections, but rely on a significant decrease in synaptic input. Previous work reported substantial
392 change in the cortical representation of the conditioned tastant in GC following aversive learning
393 (Yasoshima and Yamamoto, 1998; Accolla et al., 2007; Grossman et al., 2008). Our work provides
394 novel evidence regarding the circuit mechanisms underlying this reorganization process and
395 identifies long term plastic changes associated with CTA.
396
397 **CTA and immediate early gene expression**
398 The behavioral paradigm we used consisted of two rounds of conditioning with taste-malaise
399 pairing to ensure reliable expression of aversion learning. As a readout of the aversive memory,
400 we used a 2-bottle test to determine volume consumption of the conditioned stimulus following
401 learning, and to compute the aversion index between control and CTA animals. The 2-bottle test
402 did not initiate an extinction process, as we show that the aversion index remained stable when

403 animals were tested on two consecutive days. Quantification of IEGs, as a proxy for GC neurons'
404 activity, showed reduced expression of both c-Fos and EGR1 following testing in CTA animals
405 compared to control. The decrease in IEG expression provides additional support as to the lack of
406 extinction initiation, as extinction has been shown to increase IEG expression in GC (Hadamitzky
407 et al., 2015).
408 In our paradigm, all animals, including controls, are exposed to sucrose twice. While for CTA
409 animals sucrose is always associated with a gastric malaise, in control animals sucrose is a safe,
410 palatable stimulus and animals consume it more than water. In control animals, the consumption
411 of sucrose on the second exposure is higher than the first, consistent with attenuation of neophobia
412 (Lin and Reilly, 2012) in control rats, an effect that is associated with a reduction in c-fos
413 expression in GC (Lin et al., 2012). In the CTA group, the consumption of sucrose at the second
414 exposure was significantly lower than in the first. The differences in IEG expression we report
415 may reflect a blunted GC activation to sucrose in CTA animals compared to control. Consistent
416 with this possibility, previous studies showed increased IEG expression in the insular cortex
417 following consumption of a novel tastant alone (saccharine), but not in response to a LiCl injection
418 alone (Wilkins and Bernstein 2006; Bernstein and Koh, 2007). Thus, our data support the
419 interpretation that the decrease in IEG expression are due to animals in the CTA group expressing
420 an aversion to sucrose, rather than the control group learning that sucrose is "safe". As c-fos
421 expression is considered a proxy for activity, our results are consistent with previously published
422 work showing reduced spiking activity of GC neurons in the palatability epoch following CTA
423 (Grossman et al., 2008; Piette et al., 2012). Thus, the aversive memory induced by our behavioral
424 paradigm was reliable, allowing us to assess the effects of CTA on the BLA-GC circuit.
425

426 **CTA reduced excitatory synaptic drive onto GC neurons**

427 Our analysis of synaptic and intrinsic properties of GC neurons allowed us to parse apart which of
428 these components was responsible for the reduction in GC activity seen with CTA. We show that
429 excitatory spontaneous synaptic charge onto GC pyramidal neurons is reduced following CTA, an
430 effect that points to widespread modulation of synaptic transmission in GC, indicating that CTA
431 affects the circuit in GC broadly. CTA altered synaptic drive and capacity for plasticity at BLA-
432 GC synapses, effects consistent with chnges in the activation of GC. These results strongly suggest
433 that decreased synaptic drive onto GC neurons underlie the CTA-dependent circuit reorganization
434 reported in previous work (Accolla and Carleton, 2008) and explain the reduced firing rates of GC
435 neurons following CTA (Grossman et al., 2008).

436 Analysis of spontaneous excitatory synaptic events revealed significant decreases in amplitudes,
437 and no changes in frequency. These effects are consistent with a postsynaptic site of expression of
438 CTA-dependent modifications of synaptic efficacy (Malinow and Malenka, 2002; Rumpel et al.,
439 2005). Further confirmation of the postsynaptic site of expression comes from analysis of BLA-
440 evoked responses onto GC pyramidal neurons. Following CTA, we observed a significant decrease
441 in the amplitude of BLA-EPSCs and BLA-EPSPs, but no change in their paired pulse ratio.
442 Furthermore, the lack of changes in intrinsic excitability indicate that the profound effects taste
443 aversion learning has on GC pyramidal neurons is via modulations at specific synaptic inputs and
444 not an alteration in intrinsic membrane properties. Together, this set of findings confirm the central
445 role of the BLA-GC connection in CTA learning, and demonstrates a role for plasticity of BLA-
446 evoked synaptic responses onto L2/3 pyramidal neurons in this form of hedonic learning.

447

448 **Postsynaptically expressed LTD at amygdalocortical synapses as a mechanism for CTA**

449 When we compared the effect of CTA on two different forms of LTD, induced by patterns of
450 stimulation designed to mimic BLA neurons' activity in different behavioral states (Fontanini et
451 al., 2009; Parsana et al., 2012), we found a selective occlusion of plasticity induced by a phasic
452 pattern of activity. Phasic stimulation induced a postsynaptically expressed form of LTD in control
453 rats, but LTP in the CTA group, suggesting that phasic LTD and CTA share common mechanisms.
454 The occlusion was specific to the phasic induction pattern, as LTD induced with a tonic pattern of
455 BLA terminal field activation, a form of LTD with a presynaptic site of expression, was not
456 affected by CTA. These results point to postsynaptic LTD at BLA-GC synapses as a mechanism
457 for taste aversion learning.
458 The underlying mechanisms of postsynaptically expressed LTP and LTD have been studied
459 extensively. Signaling cascades leading to the regulation of AMPA receptors in the postsynaptic
460 membrane are thought to mediate changes in synaptic efficacy (Malinow and Malenka, 2002;
461 Kessels and Malinow, 2009). Current thinking associates learning with an increase in synaptic
462 efficacy (Bliss and Collingridge, 1993; Rogan et al., 1997; Dityatev and Bolshakov, 2005), and
463 changes in molecular markers for plasticity following CTA have been interpreted as indication of
464 LTP expression (Shema et al., 2007; Gal-Ben-Ari and Rosenblum, 2011). However, many of the
465 molecular mechanisms involved in CTA (Berman and Dudai, 2001; Gal-Ben-Ari and Rosenblum,
466 2011; Guzman-Ramos and Bermudez-Rattoni, 2012) can be engaged by both LTP and LTD
467 (Yilmaz-Rastoder et al., 2011; Gandolfi et al., 2017; Li and Pozzo-Miller, 2019). Additional
468 evidence in support of the interpretation that CTA should potentiate BLA input to GC came from
469 studies based on BLA activation with drug infusions or tetanic electrical stimulation during CTA
470 learning. Local field potential (LFP) recordings in GC of anesthetized rodents showed that the
471 induction of LTP of the population signal evoked by tetanic stimulation of the amygdala was

472 occluded by CTA (Escobar and Bermudez-Rattoni, 2000; Escobar et al., 2002), suggesting that
473 plasticity at the BLA input to GC may play a role in this learning paradigm. However, this
474 experimental design does not assess whether the baseline response has been affected by CTA, nor
475 which component of the population signal has been modified by CTA. Furthermore, these data do
476 not indicate whether LTP at BLA-GC synapses may be sufficient for learning.
477 A key feature of our study that distinguishes it from previous work is the use of optogenetic
478 techniques to selectively activate BLA terminal fields within GC. By using this approach we
479 avoided the confound of recruiting BLA collaterals to other areas which inevitably occurs with
480 somatic activation of BLA neurons. Furthermore, our study is the first to examine baseline
481 synaptic transmission, and therefore may yield different results from field potential recordings,
482 which lack synaptic resolution, and are difficult to interpret as the circuit components that
483 contribute to the LFP trace in GC have not been described (Escobar and Bermudez-Rattoni, 2000;
484 Escobar et al., 2002; Rodriguez-Duran et al., 2011). No analysis of changes in synaptic efficacy
485 has been reported up to the present work. In view of our results demonstrating a reduction in the
486 efficacy of BLA glutamatergic synapses onto GC neurons following CTA, it is likely that in L2/3
487 pyramidal neurons, signaling mechanisms for LTD are recruited during CTA.
488

489 **LTD at amygdalocortical synapses in GC is sufficient for the induction of CTA**

490 Association of sucrose and phasic stimulation of BLA terminal fields in GC *in vivo* was sufficient
491 to induce a weak CTA, unveiled as a reduction in sucrose consumption during the 2-bottle test. In
492 these experiments, the phasic pattern of stimulation was delivered after sucrose in place of LiCl,
493 thus selectively activating the BLA-GC input in the absence of a gastric malaise. Our results
494 indicate that the pattern of activity for LTD at BLA-GC synapses is sufficient to change the

495 hedonic value of sucrose. While activation of BLA-GC terminal fields *in vivo* was sufficient for
496 changing the valence of sucrose, it did not induce a strong aversion. This effect was expected, as
497 LiCl induces a gastric malaise that is not recruited in animals that received light stimulation
498 through the optic fiber during CTA training. GC receives extensive visceral input (Cechetto and
499 Saper, 1987) which is not activated during BLA terminal field stimulation. Furthermore, previous
500 studies have shown no change in IEG expression in the insular cortex following LiCl-induced
501 illness, suggesting that processing of information about the US primarily occurs in other parts of
502 the central gustatory system (Wilkins and Bernstein 2006; Bernstein and Koh, 2007). Our findings
503 therefore suggest that the plasticity of BLA-GC input primarily modulates the valence of a tastant,
504 and that integration of other sources of information about the US may be necessary for eliciting a
505 strong aversion.
506 Recent work has identified a role for corticoamygdala projecting neurons in CTA (Lavi et al.,
507 2018; Kayyal et al., 2019), suggesting that this population of GC neurons is involved in the
508 acquisition and retrieval of the aversive taste memory. Whether the population of amydala-
509 projecting and amygdala-recipient neurons in GC overlap is currently unknown, but this study
510 raises interesting questions about how and when reciprocal connections between BLA and GC are
511 recruited in CTA. It is also unclear whether amygdalocortical neurons in GC project exclusively
512 to BLA, or also interact with other nodes of the CTA circuit.
513

514 **Conclusion**

515 LTD was proposed as a mechanism for learning in cerebellar circuits (Ito et al., 2014; Hirano et
516 al., 2016) and is thought to contribute to the control of alcohol seeking behavior in the basal ganglia
517 (Ma et al., 2018). In both circuits, LTD is induced at glutamatergic synapses onto GABAergic

518 neurons (Hansel and Linden, 2000; Kakegawa et al., 2018), providing a form of disinhibition to
519 the downstream synaptic targets. Our study focused on plasticity of BLA input onto excitatory
520 neurons in L2/3 of GC, strongly supporting a role for LTD at glutamatergic synapses onto
521 pyramidal neurons in hedonic learning.

522 To our knowledge, our results are the first to directly assess the effect of CTA on BLA-GC
523 synapses, and provide the first evidence for a direct link between LTD of amygdalocortical
524 transmission onto GC neurons and taste aversion learning. Taste circuits are highly conserved
525 among species, and changes in taste preference can be induced similarly in humans as well as
526 many other organisms, making CTA and the amygdalocortical system ideal models for
527 investigating neural mechanisms of hedonic learning. Our results link LTD at the BLA-GC input
528 to a change in taste preference, emphasizing how changes in synaptic efficacy underlie adaptive
529 shifts in hedonic value capable of influencing perception and behavior.

530

531 **Methods**

532 Long Evans rats of both sexes were used for this study. Animals were singly housed in a vivarium
533 on a 12h/12h light dark cycle with ad libitum access to food and water, except where otherwise
534 noted. Experiments were conducted during the light period. All surgical and experimental
535 procedures were approved by the Institutional Animal Care and Use Committee of Stony Brook
536 University and followed the guidelines of the National Institutes of Health.

537 *Conditioned taste aversion training*. Rats were placed on water restriction with free access to food
538 for a total of 8 days. Rats were habituated to a behavioral chamber where they had 15 min access
539 to a drinking spout with H_2O, followed by 1hour access to H_2O in their home cage four hours later.
540 The volume consumed was recorded daily throughout training (total volume (ml): juveniles, 12.58

541 ± 0.38; adults, 16.88 ± 0.72), and rats' weight was monitored to ensure that it remained within
542 85% of initial weight. Four days of habituation training was sufficient to stabilize fluid intake
543 levels (Habituation, **Fig. 1b**). This was followed by two conditioning trials, with a recovery day in
544 between identical to the habituation days. The recovery day enabled us to confirm that the
545 conditioning procedures did not affect thirst levels. For immunohistochemistry and slice
546 electrophysiology, conditioning consisted of 15 min access to a drinking spout with 0.1 M sucrose,
547 followed by an ip injection of 0.15 M LiCl (7.5 mL/kg) to induce gastric malaise. Rats in the
548 control group received an ip LiCl injection (0.15 M) in the evening on day 4 and 6 of training. The
549 injection was delivered approximately 16 hours before sucrose presentation to ensure lack of
550 association between gastric malaise and sucrose consumption (**Fig 1a**, pseudo CTA). For
551 experiments *in vivo*, conditioning consisted of 15 min access to a drinking spout with 0.1 M
552 sucrose, followed by optogenetic stimulation of BLA terminal fields in GC. On the 8th training
553 day, all groups engaged in a 2-bottle test to assess a preference for H_2O or sucrose. In a subset of
554 experiments, the 2-bottle test was repeated on day 9, to assess whether the first test had initiated
555 an extinction process (**Fig. 2**).
556 *Immunohistochemistry.* Detection of immediate early gene expression - One hour after the 2-bottle
557 test, rats were anesthetized and intracardially perfused with PBS followed by 4%
558 paraformaldehyde in PBS (4% PFA). The brain was dissected out and thin (50µm) coronal slices
559 containing GC were cut with a fixed tissue vibratome (Leica VT1000). Sections were washed in
560 PBS (3 x 10 min rinse), permeabilized and blocked in a solution containing 0.5% Triton X and
561 10% normal goat serum in PBS for 1 h, then incubated overnight at 4°C in a solution containing
562 0.1% Triton X and 3% normal goat serum in PBS, mouse anti-GAD67 (1:500, MilliporeSigma,
563 MAB5406, monoclonal), and either rabbit anti-cFos (1:500, Cell Signaling, 2250S, monoclonal)

564 or rabbit anti-EGR1 (1:500, Cell Signaling, 4153S, monoclonal). Sections were then rinsed in PBS
565 (3 x 10 min) and incubated at 25°C for 2 h in a solution containing 0.1% Triton X and 3% normal
566 goat serum in PBS, goat anti-mouse Alexa Fluor-647 (1:500, Invitrogen, A21235), goat anti-rabbit
567 Alexa Fluor-568 (1:500, Invitrogen, A11011), and NeuroTrace 435/455 (1:1000, Invitrogen,
568 N21479). After a final wash in PBS (3 x 10 min), sections were mounted with Fluoromount-G
569 (Southern Biotech). Sections were imaged with a confocal microscope (Olympus Fluoview) at 20x
570 magnification. Four sections, spaced at 200 µm, were counted per animal for each IEG (cFos = 4,
571 EGR1 = 4) using ImageJ software by a person blind to experimental condition. Cell counts
572 represent the number of IEG-positive, GAD67-negative neurons, normalized by the counting area
573 (L2/3 aGC) for each section.
574 Recovery of recorded neurons in acute slice preparation - Recorded slices were fixed in 4% PFA
575 for 1 week. They were then washed in PBS (3 x 10 min rinse), permeabilized and blocked in a
576 solution containing 1% Triton X and 10% normal goat serum in PBS for 2 h, then slices were
577 incubated overnight at 4°C in a solution containing 0.1% Triton X and 3% normal goat serum in
578 PBS, streptavidin Alexa Fluor-568 conjugate (1:2000, Invitrogen, S11226), mouse anti-GAD67
579 (1:500, MilliporeSigma, MAB5406, monoclonal), and chicken anti-GFP (1:1000, Abcam,
580 ab13970, polyclonal). GC slices were then rinsed in PBS (3 x 10 min) and incubated at 25°C for
581 2 h in a solution containing 0.1% Triton X and 3% normal goat serum in PBS, goat anti-mouse
582 Alexa Fluor-647 (1:500, Invitrogen, A21235), goat anti-chicken Alexa Fluor-488 (1:500, Abcam,
583 ab150173), and Hoechst 33342 (1:5000, Invitrogen, H3570). BLA slices were incubated overnight
584 at 4°C in a solution containing 0.1% Triton X and 3% normal goat serum in PBS and chicken anti-
585 GFP (1:1000, Abcam, ab13970, polyclonal). They were then rinsed in PBS (3 x 10 min) and
586 incubated at 25°C for 2 h in a solution containing 0.1% Triton X and 3% normal goat serum in

587 PBS, goat anti-chicken Alexa Fluor-488 (1:500, Abcam, ab150173), and Hoechst 33342 (1:5000,
588 Invitrogen, H3570). Validation of injection sites and positioning of fiber optics - Following
589 behavioral training, animals were anesthetized and perfused intracardially with PBS followed by
590 4% PFA. Coronal slices containing BLA and GC were cut at 100 µm with a fixed tissue vibratome
591 (Leica VT1000). All sections were washed in PBS (3 x 10 min rinse) and incubated at 25°C for 1
592 h in a solution containing 0.1% Triton X and Hoechst 33342 (1:5000, Invitrogen, H3570). Sections
593 were mounted with Fluoromount-G (Southern Biotech) and the accuracy of viral injections and
594 fiber placements was assessed.
595 *Electrophysiology*. Acute coronal slices containing GC were obtained immediately following the
596 2-bottle test. Slice preparation was as described in our previous study (Haley et al., 2016). Briefly,
597 rats were anesthetized with isoflurane (Bell jar to effect) and rapidly decapitated. The brain was
598 dissected in ice cold, oxygenated artificial cerebrospinal fluid (ACSF), and 300 µm coronal slices
599 containing GC were prepared using a fresh tissue vibratome (Leica VT1000) starting at 1.5 mm to
600 bregma. Patch clamp recordings were obtained from visually identified L2/3 pyramidal neurons
601 under DIC optics. Their identity was tested online with the injection of square current pulses (700
602 ms) to assess regular firing patterns, and post-hoc with immunohistochemistry aimed at
603 reconstructing neuron morphology, assessing location, and confirming lack of expression of the
604 GABA neuron marker GAD67. To assess possible changes in intrinsic excitability induced by
605 CTA, recordings were obtained in current clamp in the presence of fast synaptic receptor blockers
606 (in µM: DNQX, 20; APV, 50; picrotoxin, 20) and square current pulses of increasing amplitude
607 were injected to examine input resistance, action potential threshold, and frequency/intensity
608 curves. Input resistance was calculated from the linear portion of the voltage response to a -50 pA
609 current injection. Action potential threshold was calculated as the membrane voltage when the first

610 derivative of the voltage trace dV/dt = 20 V/s (Bekkers and Delaney, 2001). In a different set of
611 experiments, spontaneous synaptic activity was recorded in voltage clamp. For these experiments,
612 a cesium sulfate-based internal solution containing the sodium channel blocker QX314 (2 mM,
613 Tocris Bioscience) was used to stabilize recordings during prolonged depolarization. Spontaneous
614 excitatory synaptic currents were recorded at three different holding potentials around the reversal
615 potential for chloride (to record sEPSCs, in mV: -55, -50, -45). Current versus voltage functions
616 were used to identify the voltage that better isolated the current of interest, which were used for
617 analysis of charge and spontaneous events' amplitude and frequency (Maffei et al., 2004; Haley et
618 al., 2016). Total charge was calculated by integrating 5 s sections of the current trace. Evoked
619 EPSCs/EPSPs from stimulation of BLA terminal fields were obtained in voltage clamp and current
620 clamp using a potassium gluconate solution and holding neurons at -70mV. The monosynaptic
621 nature of BLA-EPSCs was verified as in our previous study (Haley et al., 2016). Event-triggered
622 average of light-evoked BLA-EPSCs and BLA-EPSPs was used to align BLA-EPSC and BLA-
623 EPSP onset and calculate the average amplitude of the light-evoked response. Latencies of BLA-
624 evoked responses were calculated from the onset of the phasic 5 ms light pulse. For plasticity
625 experiments, 2 LED pulses (5 ms, 10 Hz) were used to elicit BLA-EPSCs every 30 s. A brief (10
626 ms) 1 mV depolarization step was used to monitor series resistance (R_s). After a 10 min baseline,
627 either the phasic or tonic induction paradigm was applied in current clamp, after which BLA-
628 EPSCs were recorded for an additional 40 min. Neurons with R_s > 20 MΩ or that changed >10%
629 during recording were excluded from analysis.
630 *Optogenetics*. *Ex vivo* experiments: Rats (P14) were anesthetized intraperitoneally with a mixture
631 containing 70 mg/kg ketamine, 0.7 mg/kg acepromazine, and 3.5 mg/kg xylazine (KXA), and
632 mounted on a stereotaxic apparatus. Animals received an injection of the AAV9.CAG.ChR2-

633 Venus.WPRE.SV40 construct ((Petreanu et al., 2007); University of Pennsylvania Vector Core)
634 in the BLA using a nanoject pressure injector (Drummond Nanoject II; 100 nL volume containing
635 5.64^{12} particles/mL) as described in our previous study (Haley et al., 2016). The stereotaxic
636 coordinates for the injections were 2.1 mm posterior to bregma; 4.7 mm lateral to midline; 7.0 mm
637 below the pia. Rats were allowed to recover from surgery for 2 weeks before CTA training and
638 recordings. AAV9 was chosen because it is primarily transported anterogradely, and because
639 ChR2 expressed via AAV9 does not alter the short-term dynamics of evoked responses (Jackman
640 et al., 2014). The lack of backfilled somata in all of our GC our preparations further confirms
641 forward direction of transport and indicates that only BLA terminal fields in GC were activated by
642 light pulses. Consistency of ChR2-Venus expression across preparation was as previously reported
643 (Haley et al., 2016). Briefly, as shown in **Fig. 4b**, the intensity of the Venus signal in GC was
644 quantified across a 500um wide region of interest (ROI) spanning the cortical mantle from the pia
645 to L5/6 (included) across 10 preparations. The average and standard deviation of the fluorescent
646 signal were plotted as a function of depth. The expression of the Venus signal was then assessed
647 for all preparations used for electrophysiological recordings and compared to the calibration curve.
648 Only data obtained from preparations with a fluorescence profile within 1 standard deviation of
649 the average calibration curve were included in the analysis.
650 BLA-EPSCs were evoked with a 5ms light pulse delivered through the 40x objective mounted on
651 an upright microscope (Olympus BX51WI). The intensity, frequency and timing of the blue light
652 stimuli (470 nm) were controlled with an LED driver (ThorLabs). Intensity at the output was
653 verified with a light meter (Thor Labs, Range: 0.2 - 4.4 mW). Phasic stimulation for plasticity
654 induction was organized in 20 trains of 20-5 ms light pulses at 20 Hz delivered every 250 ms and
655 paired with depolarization of the postsynaptic neuron with a 50 pA current step. Tonic activation

656 of BLA terminal fields was achieved using a ramping light stimulus (which prevented inactivation
657 of ChR2 channels (Lin et al., 2009). The duration of the ramping stimulus was 6 s from 0 to
658 maximum (4.4 mW) light intensity and was controlled through the LED driver connected to an
659 analog output of the amplifier. For plasticity induction, 10 ramping stimuli spaced 5 s were (**Fig.**
660 **6**) paired with depolarization of the postsynaptic neuron with a 50 pA current step.
661 *In vivo* experiments: Stimulation of BLA terminal fields *in vivo* was achieved through optical
662 fibers (Doric lenses, 400 µm) chronically implanted in GC (1.4 mm anterior to bregma; 5 mm
663 lateral to midline; 4.5 mm below the pia). Rats, weighing > 250 g were anesthetized
664 intraperitoneally with the KXA cocktail described above and supplemented with 40% of the
665 induction dose as needed to maintain surgical levels of anesthesia. The scalp was exposed and
666 holes were drilled for anchoring screws, optical fibers, and viral injection. The AAV9.CAG.ChR2-
667 Venus.WPRE.SV40 construct(Petreanu et al., 2007) (University of Pennsylvania Vector Core)
668 was bilaterally injected in the BLA (3.0 mm posterior to bregma; 5 mm lateral to midline; 7.2 mm
669 below the pia) using a nanoject pressure injector (Drummond Nanoject II; 200 nL volume
670 containing 5.64^{12} particles/mL) as described above. Optical fibers (Doric Lenses, 400 µm) were
671 coated with DiI for better detection of the optic fiber tract and implanted bilaterally to target GC
672 and were secured in place with dental cement.
673 For these experiments, recovery from surgery was 4 weeks prior to CTA training. The injection
674 site in BLA and the positioning of the optic fiber in GC were verified histologically for each
675 preparation. Stimulation was controlled via the digital output of a Multi-patch clamp amplifier
676 (HEKA) and software (Patchmaster) and delivered through the implanted optical fibers coupled to
677 a blue laser (Shanghai Dream, 470 nm). Light intensity at the tip of the optic fiber was measured
678 with a light meter (6.5 mW, ThorLabs) The induction paradigm *in vivo* had the same structure as

679 the phasic induction pattern used in slices (Trains of 20 pulses, in this case 10 ms long, at 20 Hz
680 delivered every 250 ms, repeated 100 times) Animals received photostimulation immediately after
681 exposure to the 0.1 M sucrose solution on conditioning days 1 and 2. A control group of rats
682 received a BLA injection of the AAV9.hSyn.eGFP.WPRE.bGH construct (University of
683 Pennsylvania Vector Core) to ensure that possible changes in sucrose preference were due to BLA
684 terminal field stimulation and not to unspecific effects of the light stimulation.

685 *Data analysis*. Data were acquired with a HEKA 4 channels amplifier with integrated acquisition
686 board. Data were sampled at 10 kHz. Patchmaster (WaveMetrix) was used as acquisition software.
687 Analysis was performed with custom procedures in Igor (WaveMetrix), Matlab, and Clampfit
688 (Molecular Devices). Data were tested for normality, then the appropriate statistical test was
689 chosen. Where appropriate, unpaired t-tests were applied, otherwise Mann-Whitney tests were
690 applied. Multiple comparisons were assessed with OneWay ANOVA followed by post-hoc tests
691 with Bonferroni correction. Cumulative distributions were compared using the 2-sample
692 Kolmogorov-Smirnov (K-S) test. Linear regression analysis was used to determine correlations
693 between BLA-EPSC/BLA-EPSP amplitude (**Fig. 4e**, input/output function). For plasticity
694 induction experiments, paired t-tests were used to detect significant differences between BLA-
695 EPSC amplitude, PPR, and CV in the 10 min baseline period and in the 10 min period 30-40 min
696 post-induction. Differences in probability of LTD vs LTP induction following CTA were assessed
697 with χ^2 for contingency test. Significant differences were considered for $p < 0.05$.

698 *Solutions*. ACSF contained the following (mM): 126 NaCl, 3 KCl, 25 NaHCO3, 1 NaHPO4, 2
699 MgSO4, 2 CaCl2, 14 dextrose with an osmolarity of 315-325mOsm. The internal solution for
700 analysis of excitability and evoked synaptic responses was as follows (mM): 116 K-Glu, 4 KCl,
701 10 K-HEPES, 4 Mg-ATP, 0.3 Na-GTP, 10 Na-phosphocreatine, 0.4% biocytin (V_{rev} $[Cl^{-1}] = -81$

702 mV). The pH of the internal solution was adjusted to 7.35 with KOH and the osmolarity adjusted
703 to 295 mOsm with sucrose. The internal solution to assess spontaneous excitatory and inhibitory
704 charge and events contained (mM): 20 KCl, 100 Cs-sulfate, 10 K-HEPES, 4 Mg-ATP, 0.3 Na-
705 GTP, 10 Na-phosphocreatine, 3 QX-314 (Tocris Bioscience), 0.2% biocytin (Vrev [Cl−1] = −49.3
706 mV). *Drugs*. To assess the monosynaptic nature of BLA-EPSCs recordings were obtained in the
707 presence of (in μM): 1 TTX (Tocris Bioscience), 100 4-aminopyridine (4-AP) (Tocris Bioscience).
708 To determine possible changes in intrinsic excitability, the following blockers were bath applied
709 (in uM): 20 DNQX (Tocris Bioscience), and 50 APV (Tocris Bioscience), 20 picrotoxin (Tocris
710 Bioscience).

711

712 **References**

713 Accolla R, Carleton A (2008) Internal body state influences topographical plasticity of sensory
714 representations in the rat gustatory cortex. Proc Natl Acad Sci U S A 105:4010-4015.
715 Accolla R, Bathellier B, Petersen CC, Carleton A (2007) Differential spatial representation of taste
716 modalities in the rat gustatory cortex. J Neurosci 27:1396-1404.
717 Bekkers JM, Delaney AJ (2001) Modulation of excitability by alpha-dendrotoxin-sensitive potassium
718 channels in neocortical pyramidal neurons. J Neurosci 21:6553-6560.
719 Berman DE, Dudai Y (2001) Memory extinction, learning anew, and learning the new: dissociations in the
720 molecular machinery of learning in cortex. Science 291:2417-2419.
721 Bermudez-Rattoni F, McGaugh JL (1991) Insular cortex and amygdala lesions differentially affect
722 acquisition on inhibitory avoidance and conditioned taste aversion. Brain Res 549:165-170.
723 Bliss TV, Collingridge GL (1993) A synaptic model of memory: long-term potentiation in the
724 hippocampus. Nature 361:31-39.
725 Braun JJ, Slick TB, Lorden JF (1972) Involvement of gustatory neocortex in the learning of taste aversions.
726 Physiol Behav 9:637-641.
727 Cechetto DF, Saper CB (1987) Evidence for a viscerotopic sensory representation in the cortex and
728 thalamus in the rat. J Comp Neurol 262:27-45.
729 Crozier RA, Wang Y, Liu CH, Bear MF (2007) Deprivation-induced synaptic depression by distinct
730 mechanisms in different layers of mouse visual cortex. Proc Natl Acad Sci U S A 104:1383-1388.
731 Cubero I, Thiele TE, Bernstein IL (1999) Insular cortex lesions and taste aversion learning: effects of
732 conditioning method and timing of lesion. Brain Res 839:323-330.
733 Dityatev AE, Bolshakov VY (2005) Amygdala, long-term potentiation, and fear conditioning.
734 Neuroscientist 11:75-88.
735 Escobar ML, Bermudez-Rattoni F (2000) Long-term potentiation in the insular cortex enhances conditioned
736 taste aversion retention. Brain Res 852:208-212.
737 Escobar ML, Alcocer I, Bermudez-Rattoni F (2002) In vivo effects of intracortical administration of
738 NMDA and metabotropic glutamate receptors antagonists on neocortical long-term potentiation
739 and conditioned taste aversion. Behav Brain Res 129:101-106.

740 Flynn FW, Grill HJ, Schulkin J, Norgren R (1991a) Central gustatory lesions: II. Effects on sodium appetite,
741 taste aversion learning, and feeding behaviors. Behav Neurosci 105:944-954.
742 Flynn FW, Grill HJ, Schwartz GJ, Norgren R (1991b) Central gustatory lesions: I. Preference and taste
743 reactivity tests. Behav Neurosci 105:933-943.
744 Fontanini A, Grossman SE, Figueroa JA, Katz DB (2009) Distinct subtypes of basolateral amygdala taste
745 neurons reflect palatability and reward. J Neurosci 29:2486-2495.
746 Gal-Ben-Ari S, Rosenblum K (2011) Molecular mechanisms underlying memory consolidation of taste
747 information in the cortex. Front Behav Neurosci 5:87.
748 Gandolfi D, Cerri S, Mapelli J, Polimeni M, Tritto S, Fuzzati-Armentero MT, Bigiani A, Blandini F,
749 Mapelli L, D'Angelo E (2017) Activation of the CREB/c-Fos Pathway during Long-Term Synaptic
750 Plasticity in the Cerebellum Granular Layer. Front Cell Neurosci 11:184.
751 Garcia J, Kimeldorf DJ, Koelling RA (1955) Conditioned aversion to saccharin resulting from exposure to
752 gamma radiation. Science 122:157-158.
753 Grossman SE, Fontanini A, Wieskopf JS, Katz DB (2008) Learning-related plasticity of temporal coding
754 in simultaneously recorded amygdala-cortical ensembles. J Neurosci 28:2864-2873.
755 Guzman-Ramos K, Bermudez-Rattoni F (2012) Interplay of amygdala and insular cortex during and after
756 associative taste aversion memory formation. Rev Neurosci 23:463-471.
757 Hadamitzky M, Bosche K, Engler A, Schedlowski M, Engler H (2015) Extinction of conditioned taste
758 aversion is related to the aversion strength and associated with c-fos expression in the insular
759 cortex. Neuroscience 303:34-41.
760 Haley MS, Fontanini A, Maffei A (2016) Laminar- and Target-Specific Amygdalar Inputs in Rat Primary
761 Gustatory Cortex. J Neurosci 36:2623-2637.
762 Hansel C, Linden DJ (2000) Long-term depression of the cerebellar climbing fiber--Purkinje neuron
763 synapse. Neuron 26:473-482.
764 Hirano T, Yamazaki Y, Nakamura Y (2016) LTD, RP, and Motor Learning. Cerebellum 15:51-53.
765 Inberg S, Elkobi A, Edri E, Rosenblum K (2013) Taste familiarity is inversely correlated with Arc/Arg3.1
766 hemispheric lateralization. J Neurosci 33:11734-11743.
767 Ito M, Yamaguchi K, Nagao S, Yamazaki T (2014) Long-term depression as a model of cerebellar
768 plasticity. Prog Brain Res 210:1-30.
769 Jackman SL, Beneduce BM, Drew IR, Regehr WG (2014) Achieving high-frequency optical control of
770 synaptic transmission. J Neurosci 34:7704-7714.
771 Kakegawa W, Katoh A, Narumi S, Miura E, Motohashi J, Takahashi A, Kohda K, Fukazawa Y, Yuzaki M,
772 Matsuda S (2018) Optogenetic Control of Synaptic AMPA Receptor Endocytosis Reveals Roles of
773 LTD in Motor Learning. Neuron 99:985-998 e986.
774 Kayyal H, Yiannakas A, Kolatt Chandran S, Khamaisy M, Sharma V, Rosenblum K (2019) Activity of
775 Insula to Basolateral Amygdala Projecting Neurons is Necessary and Sufficient for Taste Valence
776 Representation. J Neurosci 39:9369-9382.
777 Kessels HW, Malinow R (2009) Synaptic AMPA receptor plasticity and behavior. Neuron 61:340-350.
778 Kloc M, Maffei A (2014) Target-specific properties of thalamocortical synapses onto layer 4 of mouse
779 primary visual cortex. J Neurosci 34:15455-15465.
780 Lavi K, Jacobson GA, Rosenblum K, Luthi A (2018) Encoding of Conditioned Taste Aversion in Cortico-
781 Amygdala Circuits. Cell Rep 24:278-283.
782 Li W, Pozzo-Miller L (2019) Differences in GluN2B-Containing NMDA Receptors Result in Distinct
783 Long-Term Plasticity at Ipsilateral versus Contralateral Cortico-Striatal Synapses. eNeuro 6.
784 Lin JY, Reilly S (2012) Amygdala-gustatory insular cortex connections and taste neophobia. Behav Brain
785 Res 235:182-188.
786 Lin JY, Lin MZ, Steinbach P, Tsien RY (2009) Characterization of engineered channelrhodopsin variants
787 with improved properties and kinetics. Biophys J 96:1803-1814.
788 Lin JY, Roman C, Arthurs J, Reilly S (2012) Taste neophobia and c-Fos expression in the rat brain. Brain
789 Res 1448:82-88.

790 Ma T, Cheng Y, Roltsch Hellard E, Wang X, Lu J, Gao X, Huang CCY, Wei XY, Ji JY, Wang J (2018)
791 Bidirectional and long-lasting control of alcohol-seeking behavior by corticostriatal LTP and LTD.
792 Nat Neurosci 21:373-383.
793 Maffei A, Nelson SB, Turrigiano GG (2004) Selective reconfiguration of layer 4 visual cortical circuitry
794 by visual deprivation. Nat Neurosci 7:1353-1359.
795 Maffei A, Nataraj K, Nelson SB, Turrigiano GG (2006) Potentiation of cortical inhibition by visual
796 deprivation. Nature 443:81-84.
797 Malinow R, Malenka RC (2002) AMPA receptor trafficking and synaptic plasticity. Annu Rev Neurosci
798 25:103-126.
799 Martinez-Moreno A, Rodriguez-Duran LF, Escobar ML (2011) Late Protein Synthesis-Dependent Phases
800 in CTA Long-Term Memory: BDNF Requirement. Front Behav Neurosci 5:61.
801 Morris R, Frey S, Kasambira T, Petrides M (1999) Ibotenic acid lesions of the basolateral, but not the
802 central, amygdala interfere with conditioned taste aversion: evidence from a combined behavioral
803 and anatomical tract-tracing investigation. Behav Neurosci 113:291-302.
804 Parsana AJ, Li N, Brown TH (2012) Positive and negative ultrasonic social signals elicit opposing firing
805 patterns in rat amygdala. Behav Brain Res 226:77-86.
806 Petreanu L, Huber D, Sobczyk A, Svoboda K (2007) Channelrhodopsin-2-assisted circuit mapping of long-
807 range callosal projections. Nat Neurosci 10:663-668.
808 Piette CE, Baez-Santiago MA, Reid EE, Katz DB, Moran A (2012) Inactivation of basolateral amygdala
809 specifically eliminates palatability-related information in cortical sensory responses. J Neurosci
810 32:9981-9991.
811 Rioult-Pedotti MS, Friedman D, Donoghue JP (2000) Learning-induced LTP in neocortex. Science
812 290:533-536.
813 Rodriguez-Duran LF, Castillo DV, Moguel-Gonzalez M, Escobar ML (2011) Conditioned taste aversion
814 modifies persistently the subsequent induction of neocortical long-term potentiation in vivo.
815 Neurobiol Learn Mem 95:519-526.
816 Rogan MT, Staubli UV, LeDoux JE (1997) Fear conditioning induces associative long-term potentiation in
817 the amygdala. Nature 390:604-607.
818 Rosenblum K, Meiri N, Dudai Y (1993) Taste memory: the role of protein synthesis in gustatory cortex.
819 Behav Neural Biol 59:49-56.
820 Rumpel S, LeDoux J, Zador A, Malinow R (2005) Postsynaptic receptor trafficking underlying a form of
821 associative learning. Science 308:83-88.
822 Schiff HC, Bouhuis AL, Yu K, Penzo MA, Li H, He M, Li B (2018) An Insula-Central Amygdala Circuit
823 for Guiding Tastant-Reinforced Choice Behavior. J Neurosci 38:1418-1429.
824 Shema R, Sacktor TC, Dudai Y (2007) Rapid erasure of long-term memory associations in the cortex by
825 an inhibitor of PKM zeta. Science 317:951-953.
826 Wang L, Kloc M, Gu Y, Ge S, Maffei A (2013) Layer-specific experience-dependent rewiring of
827 thalamocortical circuits. J Neurosci 33:4181-4191.
828 Wang L, Kloc M, Maher E, Erisir A, Maffei A (2018a) Presynaptic GABAA Receptors Modulate
829 Thalamocortical Inputs in Layer 4 of Rat V1. Cereb Cortex.
830 Wang L, Gillis-Smith S, Peng Y, Zhang J, Chen X, Salzman CD, Ryba NJP, Zuker CS (2018b) The coding
831 of valence and identity in the mammalian taste system. Nature 558:127-131.
832 Yamamoto T, Fujimoto Y, Shimura T, Sakai N (1995) Conditioned taste aversion in rats with excitotoxic
833 brain lesions. Neurosci Res 22:31-49.
834 Yasoshima Y, Yamamoto T (1998) Short-term and long-term excitability changes of the insular cortical
835 neurons after the acquisition of taste aversion learning in behaving rats. Neuroscience 84:1-5.
836 Yilmaz-Rastoder E, Miyamae T, Braun AE, Thiels E (2011) LTP- and LTD-inducing stimulations cause
837 opposite changes in arc/arg3.1 mRNA level in hippocampal area CA1 in vivo. Hippocampus
838 21:1290-1301.

839

840

841

842

843